INT. J. PROD. RES., 2000, VOL. 38, NO. 4, 739–763

Three dimensional biarc approximation of freeform surfaces for machining tool path generation

YUAN-JYE TSENG†* and YII-DER CHEN†

In typical methods for machining freeform surfaces, the machining tool paths are generated by approximating the surface curves using line segments. While the approximated shape of the surface can be produced using cutters traversing along the line segments, the final surface produced may lack smoothness and continuity due to the zigzag patterns of the line segments. To reduce the difference and increase smoothness and continuity, the arc splines can be used to approximate the freeform curves and surfaces. A biarc is composed of two consecutive circular arcs with an identical tangent at the connecting point. Since the tangents at the connecting node are the same, the C^1 continuity property can be preserved. In addition, if the difference between the curvatures at the connecting node is minimized, then the C^2 smoothness property can be enhanced. In this research, the biarc segments are used to approximate the 2D and 3D freeform curves and surfaces using the largest deviation distance between the curves and the biarcs as the approximation criterion. The tool contact points generated and biarcs can be used to generate NC tool paths for machining 2D curves and 3D curves and surfaces. The methodology presented is implemented on a personal computer. Example parts modelled with B-spline curves and surfaces are tested and discussed. The test results show that the number of tool contact points and the number of segments are fewer than the typical linear approximation methods.

1. Introduction

The main idea of CAD and CAM integration is automatic generation of manufacturing information directly from CAD data. The purpose of machining tool paths is to guide the cutting tools to produce the part geometry specified in design. The typical approach to machining tool path generation can be summarized as defining a cutting logic under the constraints of tool size and part geometry to generate the tool paths within the specified tolerance.

In tool path generation for machining freeform surfaces, tool contact points are generated based on the surface definitions and the tolerance specifications. The tool contact points then are used to generate cutter location (CL) data according to the specified cutter geometry and size. The cutter location data can be post-processed to generate the NC (Numerical Control) codes for driving NC machines. In previous research in machining of freeform surfaces, there are various approaches and systems. Recent reviews can be found in Jensen and Anderson (1996) and Austin *et al.* (1997). The different methods can be summarized into four categories: (1) parametric method, (2) Cartesian method, (3) offset surface method, and (4) cubic approximation method. The parametric method has been presented by Loney and

Revision received July 1999.

† Department of Industrial Engineering, Yuan Ze University, 135 Yuan-Tung Road, Chung-Li, Taoyuan Hsien 320, Taiwan.

* To whom correspondence should be addressed. e-mail: ieyjt@saturn.yzu.edu.tw

International Journal of Production Research ISSN 0020–7543 print/ISSN 1366–588X online
http://www.tandf.co.uk/journals/tf/00207543.html

Ozsoy (1987), Choi and Jun (1989), and Elber and Cohen (1994). The parametric method generates tool contact curves by traversing along constant-parameter curves. The tool contact points are obtained by approximating the isoparametric curves with line segments. The Cartesian method generates tool paths in the *x-y-z* coordinate world. A typical Cartesian approach such as presented by Huang and Oliver (1994) generates planar equally spaced curves by intersecting parallel planes with the surface to define tool contact curves. The tool contact points are generated by approximating the tool contact curves with line segments. The offset surface method has been presented by Kim and Kim (1995) and Tang *et al.* (1995). In the offset surface method, an offset surface is generated by offsetting with a proper distance such as a tool radius from the original surface. The tool contact points and cutter location data are generated on the offset surface using linear segment approximation. A different type of method can be characterized as cubic block approximation method. In the research by Lee *et al.* (1994) and Tseng and Sue (1999), a tool path generation method is developed for machining surfaces using an octree approximation method. A grid height approximation method is presented by You and Chu (1995), in which grid blocks with different heights are used to approximate a surface.

Based on the observation, in the previous research, machining of freeform surfaces has been performed using linear elements, for example, line segments or square blocks. As shown in figure 1(a), line segments are used to approximate a curve to produce the approximated shape of the curve or surface. While the finishing shape can be produced within the specified tolerance, the final curves and surfaces

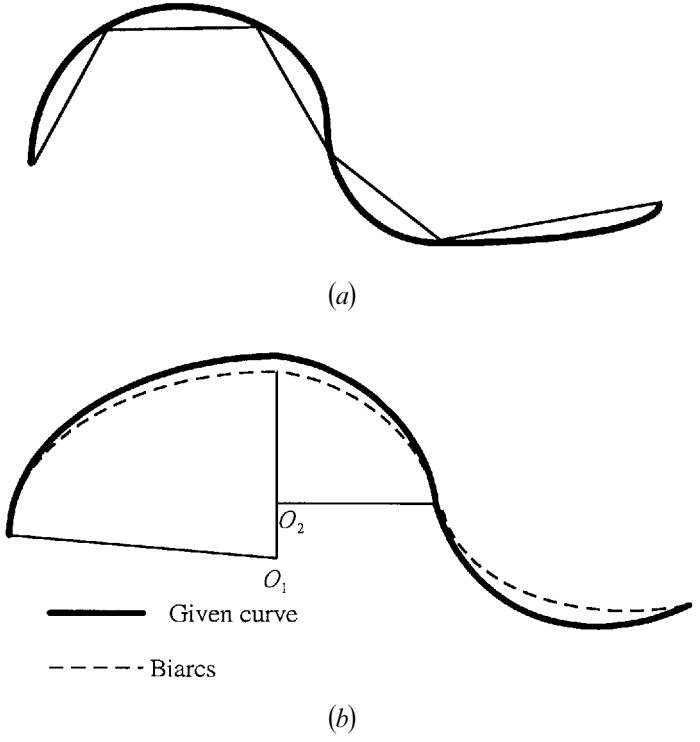

Figure 1. Approximating a curve using line segments and biarcs. (a) Approximating a curve using line segments. (b) Approximating a curve using biarcs.

produced may lack smoothness and continuity. Since the cutter actually moves in a zigzag manner, the excessive sudden changes of cutter movements may cause additional collision and tool wear. To reduce the difference and increase smoothness and continuity, arc splines can be used to approximate the curves and surfaces. Figure 1(b) shows an example of approximating a curve using biarcs.

A biarc is composed of two connected circular arcs with the identical tangent direction at the connecting point. Since the tangents at the connecting point are the same, the tangent continuity property can be preserved. In addition, if the difference between two curvatures at the connecting point is minimized, then the smoothness property can also be enhanced. Furthermore, line segments and single circular arcs are all special cases of biarcs. Therefore, the alternatives in determining the most appropriate biarc segments for approximating a given curve are unrestricted. The traditional line segment approximation can be considered a special case in the biarc approximation. Based on this idea, the biarc segments can be used to approximate the curves and surfaces to achieve the purpose of C^1 tangent continuity and C^2 curvature continuity. The biarcs are suitable for generating machining tool path, since all the NC machines are equipped with circular interpolating capability. Proper NC codes can be assigned to guide the cutters to traverse the circular arcs. In this research, new methods are developed to generate tool contact points and paths for machining 3D freeform curves and surfaces using the biarc approximation approach.

The biarcs have been applied in fitting and approximating discrete data points in previous research such as presented in Parkinson and Moreton (1991), Moreton *et al.* (1991), Meek and Walton (1992), Schonherr (1993), and Yeung and Walton (1994). In the related research in biarc fitting and approximating a given curve, Meek and Walton (1993) uses biarc to approximate a 2D quadratic curve. Biarcs are used to build bounds for a given curve. The bounded regions are used to evaluate the tolerance between the biarcs and the given curve. In Ong *et al.* (1996), an approach to biarc fitting of 2D B-spline curves is presented. The objective is to minimize the area between the biarcs and the curve. Although the area can be minimized, the important tolerance specifications such as the absolute deviation distance may be out of range. In common machining practice, the tolerance is usually specified as the largest deviation distance between the tool path and the designed curve.

In summary, in previous research, biarcs have been used in approximating and fitting a group of data points. In addition, biarcs have been used in approximating and fitting 2D curves. However, biarcs have not been used in approximating 3D curves and 3D surfaces. Moreover, the tolerances are not discussed from the machining point of views. The commonly used deviation distance has not been used as the approximating criterion. Therefore, a general 3D biarc approximation model is required for approximating 3D curves and surfaces for machining purposes.

In this research, a new approach is presented for tool path generation for machining 3D curves and surfaces using biarc approximation. First, 2D biarcs are used to approximate a 2D B-spline curve. Second, a new model of 3D biarcs is presented for approximating a 3D B-spline curve. Third, 3D surface curves are approximated using biarcs for generating tool contact points and paths for machining 3D surfaces. The approximating criterion is the largest allowed deviation distance between the curve and the biarcs. The biarcs generated define the tool contact points and paths. The tool contact points and paths can be post-processed for NC code generation for machining. The 2D biarcs are suitable for machining on a 3-axis

milling machine. The 3D biarcs are suitable for machining on a 5-axis machine tool. The 3D surfaces can be machined by machining the 2D surface curves, if the surface curves are generated using the Cartesian planar section method. The 3D surface can be machined by machining the 3D surface curves, if the surface curves are generated using the isoparametric method.

In the following section, the methods for biarc approximation of 2D curves and 3D curves are presented. In § 3, tool path planning for machining 3D surfaces using 3D biarc approximation is discussed. Section 4 presents the implementation and discussions. Finally, § 5 concludes this study.

2. Biarc approximation of 3D curves

2.1. *2D biarcs*

A biarc can be described as two circular arcs connected at a point. Also, at the connecting point, the tangents of the two circular arcs are the same. As shown in figure 2, the points S and E are the start point and end point of the biarc. The point Q is the connecting point of the two circular arcs C_S and C_E. The tangents at the connecting point are the same.

As shown in figure 3, the line SE is built by connecting the start point and end point. The angle $\alpha\left(-\pi < \alpha < \pi\right)$ represents the tangent angle measured from tangent t_S to line SE. The angle $\beta\left(-\pi < \beta < \pi\right)$ represents the tangent angle measured from the line SE to the tangent t_E. As shown in figure 3, the arc angles θ and γ can be measured at the centres O_S and O_E. If the start point S, end point E, tangent t_S at S, tangent t_E at E, and the angles α and β are known, then the arc angles θ and γ can be calculated.

In figure 3, it can be observed that $\alpha + \beta = \theta + \gamma$. Therefore, it can be obtained that $\gamma = \alpha + \beta - \theta$, where $\theta\left(-\pi < \theta < \pi\right)$ denotes the arc angle of arc C_S, and $\gamma = \alpha + \beta - \theta\left(-\pi < \gamma < \pi\right)$ denotes the arc angle of arc C_E. An arc angle is measured from the start point to the end point. If an arc angle is measured in an anti-clockwise direction, it is designated a positive angle. If an arc angle is measured in clockwise direction, it is designated a negative angle.

2.2. *Different cases of biarcs*

The special shapes of biarcs can be identified according to the different relationships between the tangent angles α and β. Several special cases can be recognized.

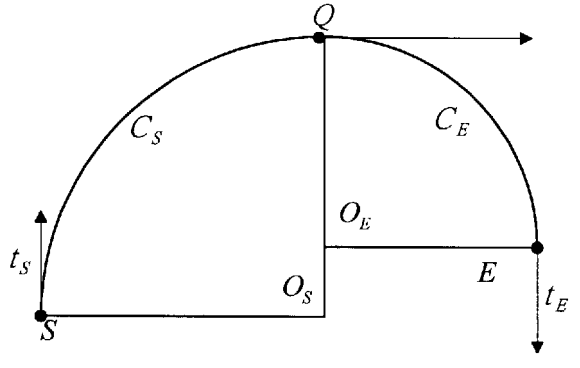

Figure 2. Illustrations of the shape and the definitions of a biarc.

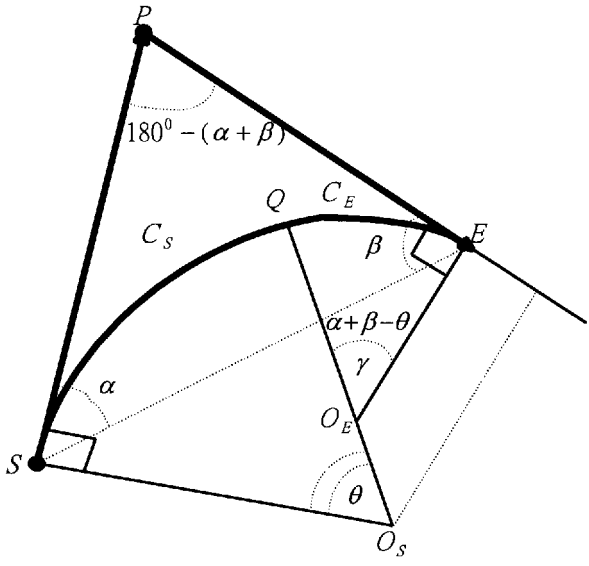

Figure 3. Illustrations for determining the arc angles θ and γ for a biarc.

For example, a line segment is a special case of biarcs. A single circular arc is also a special case of biarcs. Therefore, there are various alternatives in determining the most suitable shapes of biarcs for approximating a given curve. This is illustrated in figure 4 and the different cases are listed as follows.

(1) $\alpha = \beta = 0$
The biarc is a line segment, as shown in figure 4(a).
(2) $\alpha = \beta \neq 0$
The biarc is a single circular arc, as shown in figure 4(b).
(3) $\alpha \neq 0$ and $\beta \neq 0$
This is the general case of a biarc, as shown in figure 4(c).
(a) If θ and γ have the same sign, then the biarc is C-shape.
(b) If θ and γ have different signs, then the biarc is S-shape.

2.3. *3D biarcs*

In this research, the new idea of 3D biarcs is presented. The definitions of 3D biarcs are modelled and are utilized to approximate 3D curves and 3D surfaces. A 3D biarc is composed of two 2D biarcs twisted in space. As shown in figure 5, two 2D biarcs lie on two different planes and are connected at a point on the intersecting line of the two planes. The first biarc B_S lies on the first osculating plane P_1. The second biarc B_E lies on the second osculating plane P_2. The intersection of the two osculating planes P_1, and P_2 is the line segment *ab*. The two biarcs are connected at the point Q lying on the line segment *ab*. The line segment *ab* represents the tangent direction at the connecting node. The 3D biarc can be defined by the two biarcs B_S and B_E connected at the point Q where the tangents are identical.

As shown in figure 5, there exists a twist angle σ between the two osculating planes P_1 and P_2. The twist angle σ can be used to verify the 2D biarcs and 3D biarcs. In this way, the 2D biarcs and 3D biarcs can be represented using one single

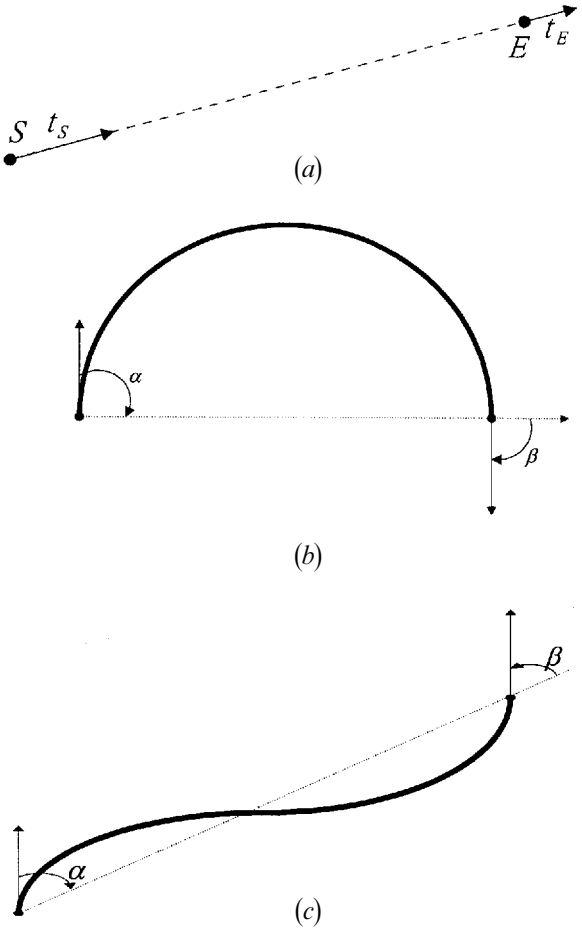

Figure 4. The different cases of special shapes of biarcs. (a) When $\alpha = \beta = 0$, the biarc is a line segment. (b) When $\alpha = \beta \neq 0$, the biarc can be represented as a single circular arc. (c) The general case of a biarc.

model. If the angle $\sigma = 0$, then it is a 2D biarc. If the angle $\sigma \neq 0$, then it is a 3D biarc. This is illustrated in figure 5 and is summarized as follows.

If the twist angle $\sigma \neq 0$, then it is a 2D biarc.
If the twist angle $\sigma \neq 0$, then it is a 3D biarc.

As shown in figure 6, the connecting point lies on the line segment defined by intersecting the two osculating planes. The intersecting line represents the tangent direction at the connecting point. The definition of the tangent t_Q and the connecting point Q can be calculated as follows. In figure 6, $S = (x_S, y_S, z_S)$ is the start point, $E = (x_E, y_E, z_E)$ is the end point, $t_S = (p_S, q_S, r_S)$ is the tangent at the start point, and $t_E = (p_E, q_E, r_E)$ is the tangent at the end point. The two plane equations can be given as

$$P_1(x, y, z) = a_1(x - x_S) + b_1(y - y_S) + c_1(z - z_S),$$
$$P_2(x, y, z) = a_2(x - x_E) + b_2(y - y_E) + c_2(z - z_E)$$

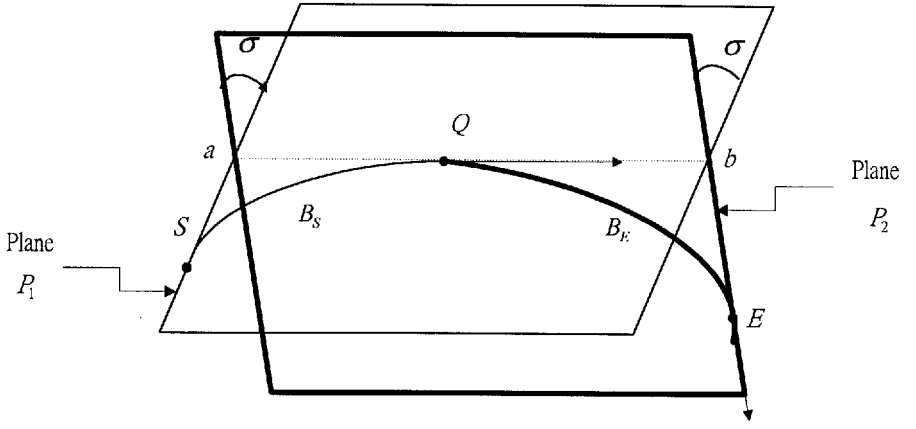

Figure 5. Illustration and definition of 3D biarcs. The first biarc B_S lies on plane P_1. The second biarc B_E lies on plane P_2.

The equations of the tangents at the start and end points can be given as

$$\frac{(x-x_S)}{p_S}=\frac{(y-y_S)}{q_S}=\frac{(z-z_S)}{r_S},$$

$$\frac{(x-x_E)}{p_E}=\frac{(y-y_E)}{q_E}=\frac{(z-z_E)}{r_E}.$$

The tangent t_S intersects the plane P_2 at the point a. The tangent t_E intersects the plane P_1 at the point b. Therefore, the points a and b can be solved and the tangent vector at the connecting point can be obtained as $t_Q=\overline{ab}$. Assuming $\overline{ab}=(p,q,r)$, then the line equation of line ab can be expressed as

$$\frac{x-x_1}{p}=\frac{y-y_1}{q}=\frac{z-z_1}{r}=t, \quad \text{where } t \text{ is a real parameter, and } t\in[0,1].$$

Based on the discussions, the connecting point Q can be obtained by determining a proper parametric value of t according to a desired objective.

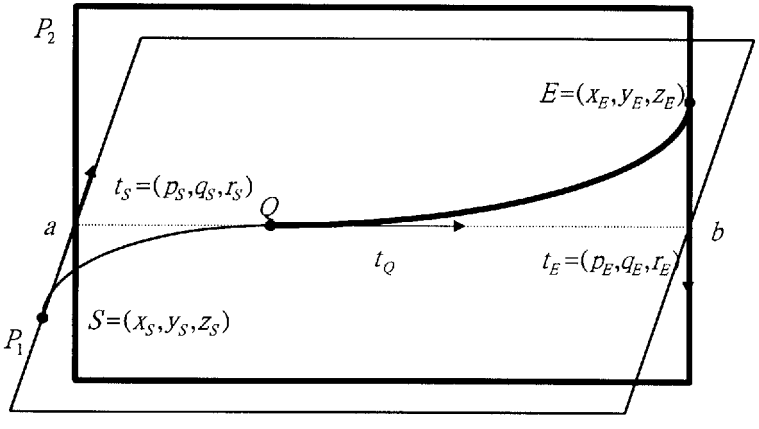

Figure 6. The connecting point and the tangent line of a 3D biarc. The connecting point Q lies on tangent line ab which is the intersection of the two planes P_1 and P_2.

2.4. *Radii of biarcs*

2.4.1. *Radii of 2D biarcs*

If the tangent angles α and β are known, then the radii of the biarc can be determined. Figure 7 shows a 2D biarc starting at point S and ending at point E. The radius of the first circular arc is denoted as r_S and the radius of the second circular arc is denoted as r_E. Assuming the centres O_S and O_E are known, then the radii of the two arcs can be represented as functions of α, β and θ. The relationship functions for the radii $r_S = f(\alpha, \beta, \theta)$ and $r_E = f(\alpha, \beta, \theta)$ are desired. From figure 7, it can be obtained that

$$\varphi = -\phi + \frac{\alpha + \beta}{2}.$$

Also, from ΔSQE, it can be obtained that

$$\overline{SQ} = \frac{\overline{SE}\sin(\beta - \phi)}{\sin(\alpha + \beta - \varphi - \phi)}.$$

Based on $\Delta SPO_S = \Delta QPO_S$, it can be obtained that $\theta = 2\varphi$.

In ΔSMO_S, it can be observed that $\sin\varphi = (\overline{SQ}/2)/r_A$.

Therefore, from the above equations, it can be derived that the radii of the two circular arcs of a 2D biarc are

$$r_S = \frac{\overline{SE}\sin\left(\frac{\alpha + \beta + \theta}{2} - \alpha\right)}{2\sin\frac{\theta}{2}\sin\left(\frac{\alpha + \beta}{2}\right)},$$

$$r_E = \frac{\overline{SE}\sin\left(\alpha - \frac{\theta}{2}\right)}{2\sin\left(\frac{\alpha + \beta - \theta}{2}\right)\sin\left(\frac{\alpha + \beta}{2}\right)}.$$

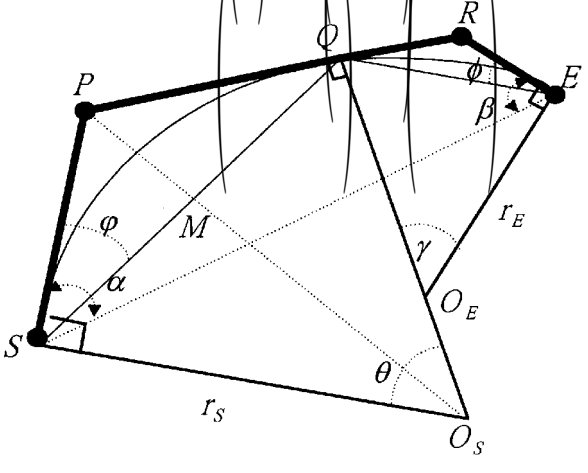

Figure 7. The illustrations for calculating the radii of a 2D biarc.

2.4.2. *Radii of 3D biarcs*

As shown in figure 8, a 3D biarc is composed of biarc SQ and biarc QE connected at the point Q. The radii of the 3D biarc can be calculated using the results derived. The radii of the first biarc are r_{S1} and r_{S2}. The radii of the second biarc are r_{E1} and r_{E2}. The four radius values of the 3D biarc can be obtained and represented as

$$r_{S1} = \frac{\overline{SQ}\sin\dfrac{\alpha+\beta+\theta_1}{2}}{2\sin\dfrac{\theta_1}{2}\sin\dfrac{\alpha+\beta}{2}}, \quad r_{S2} = \frac{\overline{SQ}\sin\dfrac{\alpha-\theta_1}{2}}{2\sin\dfrac{\alpha+\beta-\theta_1}{2}\sin\dfrac{\alpha+\beta}{2}},$$

$$r_{E1} = \frac{\overline{QE}\sin\dfrac{\alpha_1+\beta_1+\theta_3}{2}}{2\sin\dfrac{\theta_3}{2}\sin\dfrac{\alpha_1+\beta_1}{2}}, \quad r_{E2} = \frac{\overline{QE}\sin\dfrac{\alpha_1-\theta_3}{2}}{2\sin\dfrac{\alpha_1+\beta_1-\theta_3}{2}\sin\dfrac{\alpha_1+\beta_1}{2}}.$$

2.5. *Arc angles of biracs*

2.5.1. *Arc angles of 2D biarcs*

Two curvatures can be considered near identical if the difference is minimized. For a 2D biarc case, if the curvatures of the two circular arcs of a biarc are almost the same, then the curvature continuity can be enhanced. The arc angles of the two circular arcs of a biarc can be determined based on the objective of minimizing the difference between two curvatures. From the equations of r_S and r_E, the curvatures K_S and K_E of the two circular arcs can be obtained. To minimize the difference $K_{\text{diff}} = |K_S - K_E|$, the following calculation is developed.

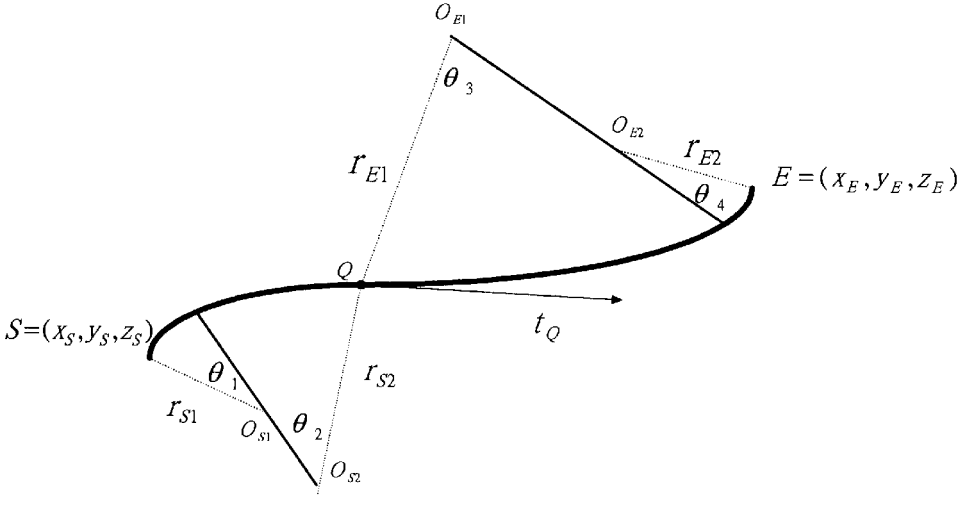

Figure 8. The illustration of arc angles and radii of a 3D biarc.

$$K_{\text{diff}} = \frac{2\sin\frac{\alpha+\beta}{2}}{\overline{SE}}\left[\frac{\sin\varphi}{\sin\left(\varphi-\frac{\alpha}{2}+\frac{\beta}{2}\right)}-\frac{\sin\left(-\varphi+\frac{\alpha+\beta}{2}\right)}{\sin(\alpha-\varphi)}\right]$$

Therefore, K_{diff} can be minimized by solving $\partial K_{\text{diff}}/\partial\varphi = 0$.

As a result, it can be derived that when $\theta = 2\varphi = (3\alpha - \beta)/2$, the difference between two curvatures is minimized.

2.5.2. *Arc angles of 3D biarcs*

From the results of the 2D case, the arc angles of 3D biarcs can also be determined based on the objective of minimizing the difference in curvatures. As shown in figure 8, the 3D biarc is composed of biarcs SQ and QE connected at the point Q. The arc angles of the 3D biarcs can be represented as

$$\theta_1 = \frac{3\alpha - \beta}{2} \quad \text{and} \quad \theta_2 = \alpha + \beta - \theta_1,$$

$$\theta_3 = \frac{3\alpha_1 - \beta_1}{2} \quad \text{and} \quad \theta_4 = \alpha_1 + \beta_1 - \theta_3.$$

2.6. *Centres of biarcs*

2.6.1. *Centres of 2D biarcs*

From the above discussions, the radii and tangents of a biarc can be obtained. The centres of the biarc are to be determined. As shown in figure 9, with the known start point $S = (x, y)$, tangent $t_S = (x_S, y_S)$, and radius R, there are two possible centres, $O_1(x_1, y_1)$ and $O_2(x_2, y_2)$. As shown in figure 10, it is observed that the correct centre can be determined based on the magnitudes of $\Delta\omega_1$ and $\Delta\omega_2$. Given the connecting point $Q = (x_q, y_q)$, by traversing a step of Δq, the magnitudes of $\Delta\omega_1$ and $\Delta\omega_2$ can be calculated as

$$\Delta\omega_1 = \sqrt{(x_q - x_1)^2 + (y_q - y_1)^2}$$

$$\Delta\omega_2 = \sqrt{(x_q - x_2)^2 + (y_q - y_2)^2}$$

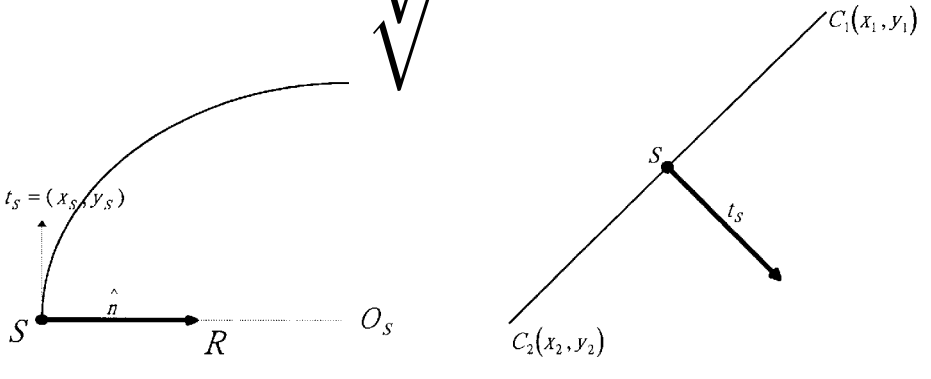

Figure 9. The illustration for finding the centres of a 2D biarc.

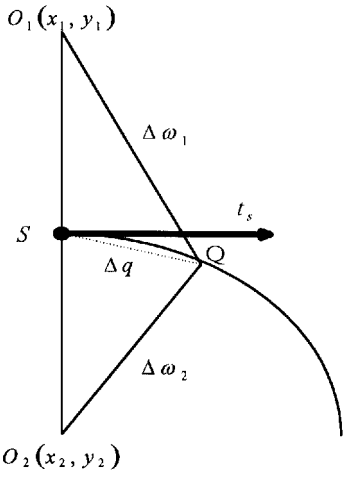

Figure 10. The illustration for determining the correct centres of a 2D biarc.

The values of $\Delta\omega_1$ and $\Delta\omega_2$ are compared. Between the two possible centres, the centre at the side with the smaller value of $\Delta\omega_1$ or $\Delta\omega_2$ is the correct centre.

2.6.2. *Centres of 3D biarcs*

For a circular arc in a 3D biarc, there are two possible centre points represented as $O_1 = (x_1, y_1, z_1)$ and $O_2 = (x_2, y_2, z_2)$, as shown in figure 11. The following values can be used to verify.

$$\Delta\omega_1 = \frac{(x_q - x_1)^2 + (y_q - y_1)^2 + (z_q - z_1)^2}{}$$

$$\Delta\omega_2 = \frac{(x_q - x_2)^2 + (y_q - y_2)^2 + (z_q - z_2)^2}{}$$

If $\Delta\omega_1 > \Delta\omega_2$, it means that $O_2 = (x_2, y_2, z_2)$ is the correct centre of arc 1 on the first plane. If $\Delta\omega_1 < \Delta\omega_2$, it means that $O_1 = (x_1, y_1, z_1)$ is the correct centre of arc 1 on the first plane. If the possible centres are O_3 or O_4 for arc 2 on the first plane, then the distance $\Delta\omega_3 = \overline{O_3 S}$ and the distance $\Delta\omega_4 = \overline{O_4 S}$ are used for verification. If $\Delta\omega_3 > \Delta\omega_4$, it means that O_4 is the correct centre of arc 2 on the first plane. If $\Delta\omega_3 < \Delta\omega_4$, it means that O_3 is the correct centre of arc 2 on the first plane. Using

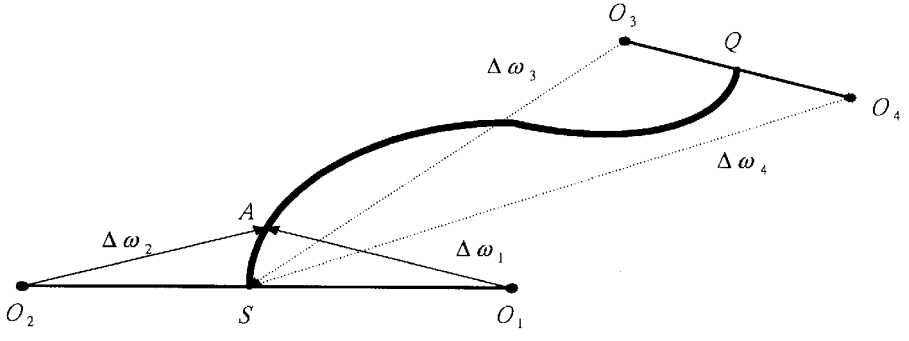

Figure 11. The illustration for determining the correct centres of a 3D biarc.

the same idea, the correct centre of arc 1 and arc 2 on the second plane can also be determined.

2.7. *Deviation distance between a curve and the approximating biarcs*

If a curve is approximated by biarcs, the deviation distance between the curve and the biarcs needs to be calculated. The deviation distance is needed in the tolerance evaluation. For a 2D case, as shown in figure 12, the points P and R are the points on a parametric curve. Given a parametric value t, the point on the curve can be obtained as $P(t) = (x_t, y_t)$. If the point P is known, then the arc angle θ_1 can be determined as follows.

If $\theta_1 < \theta$, then P is on arc C_S,
If $\theta_1 > \theta$, then P is on arc C_E.

For a 2D case, the deviation distance d between the curve and the biarc can be given as

$$d = \begin{cases} \left| \|P - O_S\| - r_S \right|, & \text{if } P \text{ is on arc } C_S, \\ \left| \|P - O_E\| - r_E \right|, & \text{if } P \text{ is on arc } C_E. \end{cases}$$

For a 3D case, if 3D biarcs are used to approximate a 3D curve, there exist a deviation distance in 3D space. As shown in figure 13(a), the biarc B_1, is on the plane P_1 and the biarc B_2 is on the plane P_2. The 3D curve RR is approximated using the 3D biarcs. As shown in the figure, there is a deviation distance d_1 between the 3D curve RR and the biarc B_1, and there is a deviation distance d_2 between the 3D curve RR and the biarc B_2. The deviation can be viewed from the direction of ab as shown in figure 13(b). The following equations can be used to calculate the deviation distance between the 3D curve and the 3D biarcs. As shown in figure 14, A_1 is a point on the 3D curve, A_2 is a point on the 3D biarc, and A_3 is the orthogonal projection of the point A_1 onto the plane P_1 of the first biarc. The centre of the biarc is O and the radius is R. Therefore, the deviation distance d can be calculated as the distance between points A_1 and A_2 and can be obtained as

$$d = \sqrt{(x_1 - x_2)^2 + (y_1 - y_2)^2 + (z_1 - z_2)^2}.$$

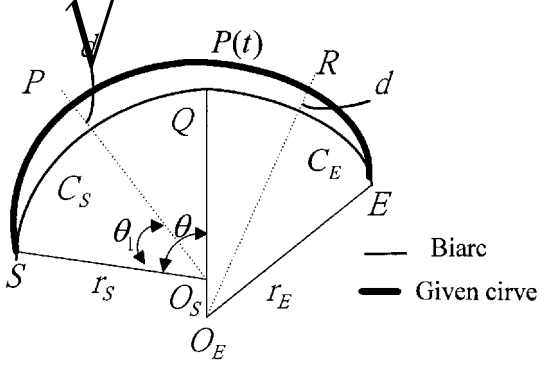

Figure 12. The deviation distance between a 2D curve and the approximating 2D biarc.

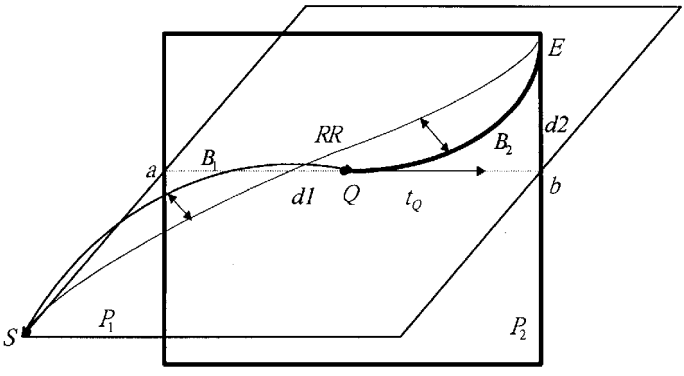

(a)

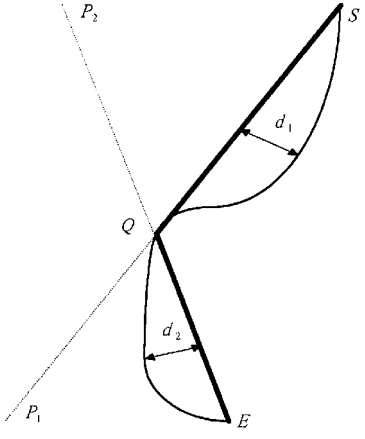

(b)

Figure 13. Illustrations of the deviation distance between a 3D curve and the approximating 3D biarc.

In implementation, the largest deviation distance d is found using an equi-interval evaluation method. The start point and the end point of a biarc are S and E. This biarc approximates a segment of curve. The two parametric values of the curve at S and E are u_S and u_E. The parametric range from u_S to u_E is divided into m_u intervals. At each of the m_u parametric value, the deviation distance between the curve and the biarc segment can be calculated as d_u. The largest deviation distance between the curve and the biarc segment can be found by comparing all the m_u intervals to find the largest $\max d_u$.

3. Tool path planning for machining surfaces using 3D biarcs

3.1. *Dividing and approximation curves*

In machining tool path generation, there is a tolerance ε specified as the largest allowed deviation distance between the curve and the tool path. If the deviation distance between the biarc and the curve is larger than the tolerance specification,

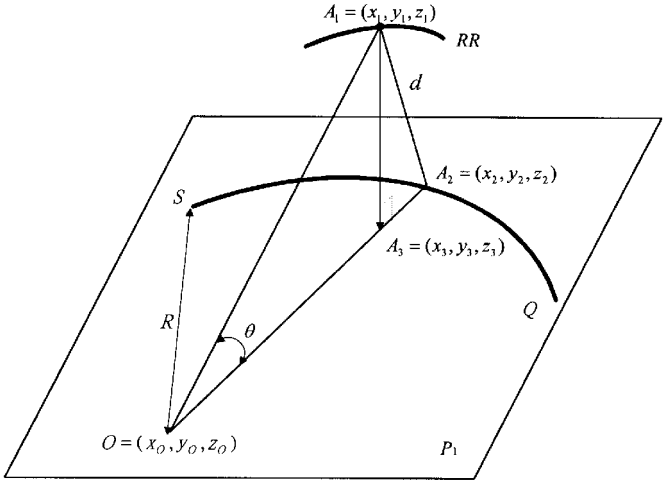

Figure 14. Calculating the deviation distance between the 3D curve and the 3D biarc.

then the curve needs to be divided. The curve can be divided into smaller segments such that each segment can be approximated by a biarc within the specified tolerance. If the divided curve segment cannot be approximated by a biarc within the specified tolerance, then the curve needs to be further subdivided. Thus, the approximation can be performed using a divide-and-approximate scheme. The biarc marks out the longest segment while maintaining the tolerance specification. Two methods can be used: (1) binary subdivision, and (2) longest arc subdivision. The binary subdivision method and the longest arc method have been used for biarc approximation of discrete data in Meek and Walton (1992). In the implementation of this research, the binary subdivision method is used in the biarc approximation of curves.

In the binary subdivision method, a B-spline curve is partitioned into two segments by dividing the parametric range into two equal intervals. Each segment of the curve is tried and approximated using a biarc segment. If the tolerance specification can be satisfied, then this segment of curve is approximated and represented by the biarc. If the tolerance specification cannot be satisfied, then this segment of curve is further subdivided into two partitions. The subdivision continues until all the segments of the curve are approximated by biarcs within the tolerance constraints. In the following divide-and-approximate algorithm, the range of the parameter of the curve is from t_0 to t_1. The tolerance ε specifies the largest allowed deviation distance between the curve and the biarcs.

Algorithm Find_Biarc2 (t_0, t_1)

(1) Approximate the curve segment (t_0, t_1) using a biarc.
The largest deviation distance is calculated as d.
(2) If $d < \varepsilon$, then the biarc is recorded,
else, calculate $t = [(t_0 + t_1)/2]$.
(3) *Find_Biarc2* (t_0, t).
Find_Biarc2 (t, t_1).
(4) end of procedure.

3.2. *Surface curve generation*

A 3D surface can be machined by moving cutting tools along surface curves. The surface curves can be generated using two methods. The parametric method generates surface curves by traversing along isoparametric curves. The generated surface curves are 3D curves. The Cartesian method generates planar equally spaced curves by intersecting parallel planes with the surface. The generated surface curves are 2D curves. In this research, the 3D surface curves can be approximated using 3D biarcs. The 2D surface curves can be approximated using 2D biarcs. Both of the 2D biarcs and 3D biarcs can be used for tool path generation.

3.3. *2D algorithms for 2D biarc approximation*

Based on the above analysis, a complete procedure of the 2D algorithm for approximating 2D B-spline curves using 2D biarcs are presented as follows.

Algorithm for 2D biarc approximation

(1) Input a 2D B-spline curve

$$p(u) = \sum_{i=0}^{n} p_i N_{i,k}(u), \quad 0 \le u \le u_{\max},$$

where p_i are the control points and $N_{i,k}$ is the B-spline function.
The start point of the B-spline is S and the end point is E.
The tolerance (largest allowed deviation distance) is specified as ε.

(2) Calculate the tangents at the points S and E as t_S and t_E.
(3) Calculate the tangent angles, α and β.
(4) Calculate the arc angles, θ and γ.
(5) Calculate the radii of the biarc as r_S and r_E.
(6) Calculate and verify the centres of the biarc as O_S and O_E.
(7) Calculate the largest deviation distance between the curve and the biarc as d.
(8) If $d \le \varepsilon$, then (a) record the biarc in a data list denoted as B,
(b) if all the segments are processed, then stop.
If $d > \varepsilon$, then (a) perform binary subdivision of the curve, and
(b) for each subdivided segment of the curve, perform (1) to (8).
(9) Output the definitions of each of the biarcs in B. The output data includes:
(a) start point $S = (x_1, y_1)$,
(b) end point $E = (x_2, y_2)$,
(c) connecting point $Q(x_q, y_q)$,
(d) centre of the biarc $O_S(x, y)$ and $O_E(x, y)$,
(e) radii of the biarc r_S and r_E.

3.4. *3D algorithms for 3D biarc approximation*

The complete procedure of the 3D algorithm for approximating 3D B-spline curves using 3D biarcs are presented as follows.

Algorithm for 3D biarc approximation

(1) Input a 3D B-spline surface

$$p(u,v) = \sum_{i=0}^{m} \sum_{j=0}^{n} p_{i,j} N_{i,k}(u) N_{j,l}(v); \quad 0 \le u \le u_{\max}; 0 \le v \le v_{\max},$$

where $p_{i,j}$ define the control polygon and $N_{i,k}$ and $N_{j,l}$ are the B-spline functions.

(2) Use isoparametric method to obtain the required 3D surface curves.
(3) For a 3D B-spline curve, the start point is S and the end point is E. The tolerance (largest allowed deviation distance) is specified as ε.
(4) Calculate the tangents at the points S and E as t_S and t_E.
(5) Calculate the tangent vector at the connecting point as $t_Q = \overline{ab}$.
(6) Calculate the tangent angles α and β of the first biarc on the first plane. Calculate the tangent angles α_1, and β_1 of the second biarc on the second plane.
(7) Calculate the arc angles of the 3D biarc.
For the first biarc on the first plane, the arc angles are obtained as

$$\theta = \frac{3\alpha - \beta}{2} \quad \text{and} \quad \alpha + \beta - \theta.$$

For the second biarc on the second plane, the arc angles are obtained as

$$\theta_1 = \frac{3\alpha_1 - \beta_1}{2} \quad \text{and} \quad \alpha_1 + \beta_1 - \theta_1.$$

(8) Calculate the radii of the 3D biarc. The four radii are obtained as r_{S1} and r_{E1}, for the first biarc, and r_{S2} and r_{E2} for the second biarc.
(9) Calculate and verify the centres of the 3D biarc as O_1, O_2, O_3, and O_4.
(10) Calculate the largest deviation distance between the 3D curve and the 3D biarc as d.
(11) If $d \le \varepsilon$, then (a) record the biarc in a data list denoted as B,
(b) if all the segments are processed, then stop.
If $d > \varepsilon$, then (a) perform binary subdivision of the curve, and
(b) for each subdivided segment of the curve, perform (1) to (11).
(12) Output the definitions of each of the 3D biarcs in B. The output data includes:
(a) start point $S = (x_S, y_S, z_S)$,
(b) end point $E = (x_E, y_E, z_E)$,
(c) connecting point $Q = (x_Q, y_Q, z_Q)$,
(d) centres O_1, O_2, O_3, O_4,
(e) radii of the 3D biarcs r_{S1}, r_{E1}, r_{S2}, r_{E2}.

4. Implementation and test results

4.1. *Tool path generation*

In a 2D case, 2D biarcs are used to approximate 2D curves. The 2D biarcs define the tool contact points and tool contact paths. If the tool geometry is defined, then the tool contact points and paths can be used to define the cutter location (CL) data for generating the required NC codes. The start point, end point, centre, and radius of each circular arc are used to define the tool path for machining the circular arcs.

In a 3D case, if the surface curves are generated using Cartesian parallel planar sections, then the surface curves are 2D curves. In this case, the 2D biarcs can be

used to approximate the 2D surface curves. After the approximation, the 2D biarcs are used to define the tool contact points and tool paths for 3-axis machining.

If the surface curves are generated using isoparametric curve generation, then the surface curves are 3D curves. The 3D biarcs are used to approximate the 3D surface curves. In the case of 3D biarcs, 5-axis machining is suitable to machine the 3D circular arcs. The 3D biarcs can be used to define the tool contact points and tool paths and generate the tool paths for used on a 5-axis machine. In implementation, the isoparametric method is used to generate the 3D surface curves while maintaining a proper cusp height between curves for machining a 3D surface.

4.2. *Examples and test results*

A test software has been implemented using the C language on a personal computer. Several example parts are modelled and tested. Two of the 2D cases are illustrated and discussed. For each part, the 2D curve is approximated using 2D biarcs. The results of 2D biarc approximation are compared with the results of line segment approximation. As shown in figure 15, the example curve A is a 2D B-spline curve built with six control points with a degree of 3. Figure 15(a) shows the results of approximating the curve A using line segments. Figure 15(b) shows the results of approximating the curve A using 2D biarcs. The two results are compared in figure 15(c). As shown in figure 15(c), three values of largest allowed deviation distance ε are tested and compared. The three values are 0.1, 0.3, and 0.5. In the case of $\varepsilon = 0{\cdot}1$, the results of line segment approximation show that the number of tool contact points is 81 and the number of segments is 80. The results of biarc approximation show that the number of tool contact points is 24 and the number of segments is 23. Consider the case in which $\varepsilon = 0{\cdot}3$, if line segment approximation is used, then the number of tool contact points is 49 and the number of segments is 48. If biarc approximation is used, then the number of tool contact points is 16 and the number of segments is 15. In the case given that $\varepsilon = 0{\cdot}5$, if line segment approximation is used, then the number of tool contact points is 35 and the number of segments is 34. If biarc approximation is used, then the number of tool contact points is 14 and the number of segments is 13.

Figure 16 shows the test results for the example curve B. The example curve B is a 2D B-spline curve built with eight control points with a degree of 4. Figure 16(a) shows the results of line segment approximation. Figure 16(b) shows the results of biarc approximation. Figure 16(c) shows the comparison between the two results. Based on the test results, it can be observed that the biarc approximation method generates a smaller number of tool contact points and fewer segments of tool contact paths.

Two of the 3D cases are illustrated and discussed. Figure 17 shows the example surface C. The example surface C is a 3D B-spline surface built with four-by-four control points. Figure 17(a) shows the results of approximating using line segments. Figure 17(b) shows the results of approximating using 3D biarcs. Figure 17(c) shows a summary and comparison of the two results. To make a more concise result, three larger values of ε are compared and presented. The three values are 1.0, 3.0, and 5.0. In figure 17(c), it shows that when $\varepsilon = 1{\cdot}0$ is tested, the results of line segment approximation show that the number of tool contact points is 343 and the number of segments is 332. The results of 3D biarc approximation show that the number of tool contact points is 217 and the number of segments is 206. The remaining data can be interpreted in the same way. Figure 18(a), (*b*), and (*c*) show

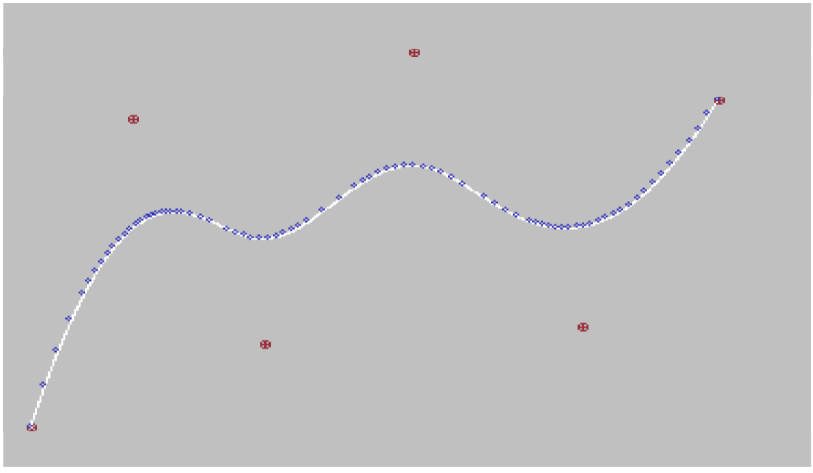

(*a*)

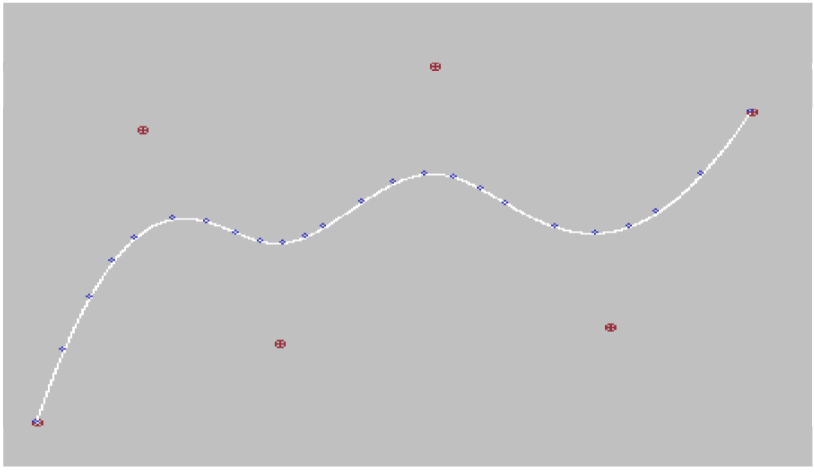

(*b*)

Curve	Control points	Degree	ε	Line segments		Biarcs	
				Points	Segments	Points	Segments
A	6	3	0.1	81	80	24	23
			0.3	49	48	16	15
			0.5	35	34	14	13

(*c*)

Figure 15. Test results of the B-spline curve A using 2D biarc approximation. Curve A control points: (110, 330) (157, 152) (218, 282) (287, 113) (365, 272) (428, 141). (a) Approximating the B-spline curve A using line segments ($\varepsilon = 0{\cdot}1$). (b) Approximating the B-spline curve A using 2D biarcs ($\varepsilon = 0{\cdot}1$). (c) Comparison of the results of approximation using line segments and biarcs.

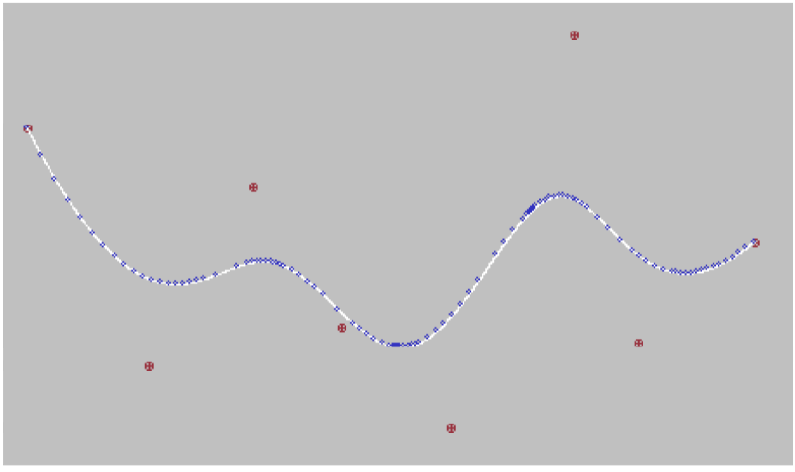

(*a*)

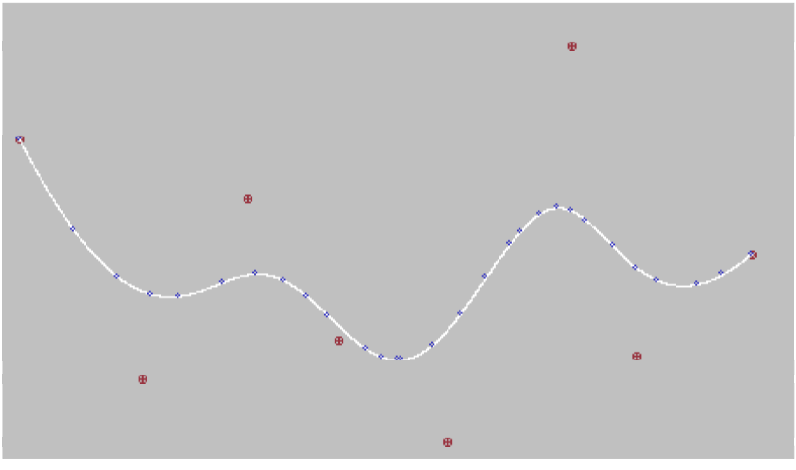

(*b*)

Curve	Control points	Degree	ε	Line segments		Biarcs	
				Points	Segments	Points	Segments
B	8	4	0.1	98	97	29	28
			0.3	64	63	21	20
			0.5	54	53	19	18

(*c*)

Figure 16. Test results of the B-spline curve B using 2D biarc approximation. Control points: (91, 166) (161, 303) (221, 200) (273, 281) (335, 339) (406, 112) (443, 290) (510, 232). (a) Approximating the B-spline curve B using line segments (ε = 0·1). (b) Approximating the B-spline curve B using 2D biarcs (ε = 0·1). (c) Comparison of the results of approximation using line segments and biarcs.

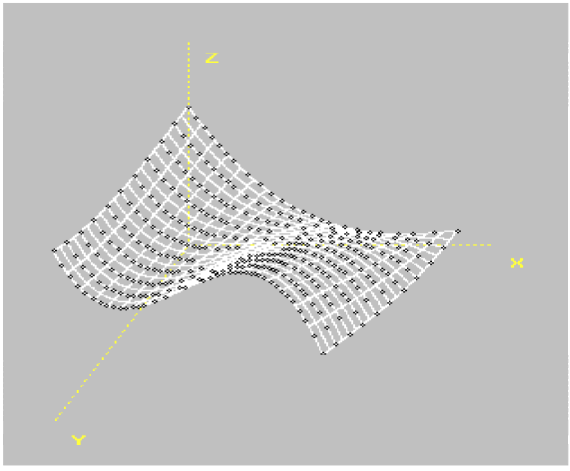

(*a*)

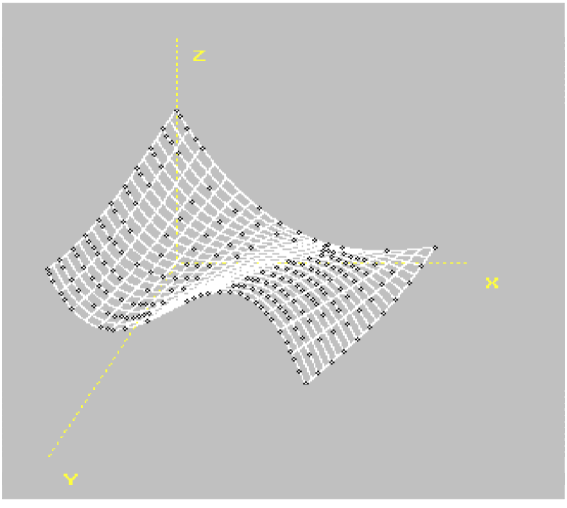

(*b*)

3D surface	Control points	Degree	ε	Line segments		Biarcs	
				Points	Segments	Points	Segments
C	4 × 4	4	1.0	343	332	217	206
			3.0	204	193	173	162
			5.0	160	149	146	135

(*c*)

Figure 17. Test results of the 3D B-spline surface C using 3D biarc approximation. Control points: (0, 0, 100) (0, 50, 100) (0, 100, 100) (0, 150, 125); (50, 010) (50, 50, 10) (50, 100, 10) (50, 150, 5); (100, 10, 10) (100, 50, 100) (100, 100, 150) (100, 150, 200); (150, 0, 10) (150, 50, 10) (150, 10, 30) (150, 150, 50). (a) Approximating the B-spline surface C using line segments (ε = 1·0). (b) Approximating the B-spline surface C using 3D biarcs (ε = 1·0). (c) Comparison of the results of approximation using line segments and biarcs.

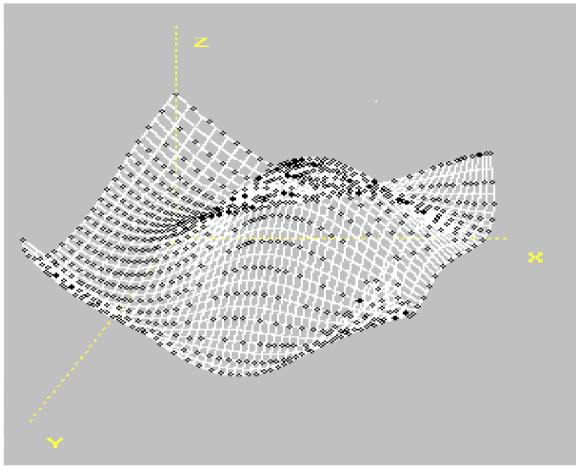

(*a*)

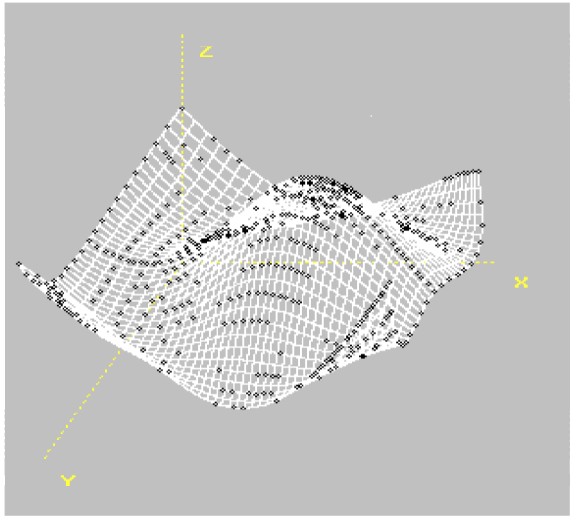

(*b*)

3D surface	Control points	Degree	ε	Line segments		Biarcs	
				Points	Segments	Points	Segments
D	5 × 5	3	1.0	766	745	420	399
			3.0	453	432	322	301
			5.0	344	323	255	234

(*c*)

Figure 18. Test results of the 3D B-spline surface D using 3D biarc approximation. (a) Approximating the B-spline surface D using line segments (ε = 1·0). (b) Approximating the B-spline surface D using 3D biarcs (ε = 1·0). (c) Comparison of the results of approximation using line segments and biarcs.

the test results for the example surface D. Based on the observation, when 3D biarc approximation is used, the number of tool contact points and the number of tool contact segments are smaller.

4.3. *Discussions*

Based on the test results, it can be observed that the biarc approximation method requires a smaller number of tool contact points and a smaller number of segments. Therefore, a general summary can be made that the biarc approximation method presents the advantages of fewer tool contact points and fewer approximating segments. Moreover, the biarc approximation method preserves the advantages of tangent continuity and curvature smoothness. Therefore, it can be summarized that the biarc approximation method is 'better' than the line segment approximation method based on the above aspects.

In 2D cases, the output data set includes the coordinates of the start point, the connecting point, the end point, the centre of the first arc, and the centre of the second arc, for each biarc. Also the output for each biarc includes the radius values of the two circular arcs. Figure 19(a) shows the output data for the example curve B. In the data set, the definitions of the 28 biarcs for approximating the curve B with $\varepsilon = 0{\cdot}1$ are listed. Figure 19(b) shows a portion of the output data for the example surface C. In the data set, the start points, end points, centres, and radii are listed. In practical machining, the presented output data format is adequate for NC code generation.

5. Conclusions

In this research, new tool path generation methods using biarc approximation are developed. In the 2D cases, 2D curves are approximated using 2D biarcs to generate the required tool contact points and paths. In the 3D cases, the 3D curves and surfaces are approximated using 3D biarcs. The biarcs mark out the largest arc length within the specified tolerance. The approximating criterion is the largest allowed deviation distance between the curves and the biarcs. By using biarc approximation, the tangent continuity can be preserved. Also, the near curvature continuity can be maintained by minimizing the difference between curvatures of the linked arcs. The new methods presented are implemented and tested using B-spline curves and surfaces with arbitrary number of control points and degrees. The test results show that the biarc approximation methods present fewer tool contact points and fewer tool path segments than the line segment approximation method. In practical machining, the generated tool contact points and paths can be used to define the NC tool paths for use on 3-axis or 5-axis milling machines or machining centre. In this research, the tool contact points and paths are generated and the output data can be used for downstream machining applications. The test results are listed but are not post processed to generate the final NC codes. Therefore, selection of cutters, determining cutter offset, and solving gouging problems are not addressed in this research. In future research, more work needs to be done on surface analysis and tool approach direction determination, cutter selection, offset calculation, and gouging avoidance in order to generate the final NC codes. In conclusion, this research presents a new method for approximating curves and surfaces using a general model of biarcs for tool path generation for the purpose of a better CAD/CAM integration.

	Starting Point		Connecting Point		End Point		Centre of Arc 1		Centre of Arc 2		Radius of Arc 1	Radius of Arc 2
	x	y	x	y	x	y	x	y	x	y	r_1	r_2
biarc 1	91	166	107.6	196.1	122.5	218.5	599.5	−93·8	346.6	53.1	571.1	278.9
biarc 2	122.5	218.5	135.5	234.3	147.3	245	281.8	100.9	106.4	168.1	198.1	97
biarc 3	147.3	245	157.6	251.6	167	255.2	190.1	189.5	177.7	212.2	70.1	44.3
biarc 4	167	255.2	175.3	256.4	183	256	177	215.9	177.1	213.3	40.5	43.1
biarc 5	183	256	196.3	252.6	207.9	248.1	174.4	196.6	6.3	−257.5	61	544.4
biarc 6	207.9	248.1	217.8	244.8	226.9	243.5	248.6	352.9	227.1	279.1	112.4	35.6
biarc 7	226.9	243.5	234.9	244.6	242.5	247.5	227.3	272.1	223.9	284.3	28.6	41.2
biarc 8	242.5	247.5	249.4	251.7	256	256.8	217.1	297.1	188.3	337.4	55.7	105.2
biarc 9	256	256.8	262	262.1	267.9	267.7	162.9	367.9	−31.1	574.9	145	428.6
biarc 10	267.9	267.7	278.7	278	289.4	286.6	−2421.1	3082.4	331	223.8	3892.7	75.4
biarc 11	289.4	286.6	294	289.4	298.7	291.5	317.3	245.6	310.7	257.8	49.6	35.7
biarc 12	298.7	291.5	303.2	292.6	307.7	293	308.5	263.1	307.1	271	30	22
biarc 13	307.7	293	308.7	292.9	309.8	292.8	309.6	336.3	307	267.8	43.3	25.2
biarc 14	309.8	292.8	318.3	290.1	327.1	284	306.4	267.2	295	247	25.8	49.1
biarc 15	327.1	284	335	276.1	343.2	266	274.1	223.1	179.9	142.8	80.7	204.6
biarc 16	343.2	266	350.5	255.9	358	245.1	105	86.7	2765	1915.7	298.1	2930
biarc 17	358	245.1	364.6	235.5	371.3	226.3	1195.1	818.8	590.8	394.5	1014.9	276.4
biarc 18	371.3	226.3	374.3	222.6	377.2	219.1	192.3	87.1	455.8	288.9	226.8	105.1
biarc 19	377.2	219.1	382,8	213.4	388.4	209.1	442.6	276.9	407.9	240.4	87.2	36.8
biarc 20	388.4	209.1	393.3	206.8	398.2	205.8	401.2	229.4	398.9	222.9	24	17.1
biarc 21	398.2	205.8	402.5	206.3	406.8	207.8	398.7	222.2	397.4	227.6	16.4	21.9
biarc 22	406.8	207.8	410.7	210.1	414.7	213.1	394	234.7	378.3	257.3	29.8	57.3
biarc 23	414.7	213.1	422.1	219.8	430	227.9	353.6	287.1	912.3	−254.4	96	682.1
biarc 24	430	227.9	436.6	234.2	443.7	240.2	580.3	78.9	500.6	165.1	211.6	94.2
biarc 25	443.7	240.2	449.6	244.2	456	247.4	486.5	182.9	473.5	204.6	71.5	46.2
biarc 26	456	247.4	466.6	250.1	478.8	249.2	470.4	211.7	470.4	212	38.4	38.1
biarc 27	478.8	249.2	485.6	247.1	492.8	243.7	468.8	204.9	462.4	189.3	45.5	62.3
biarc 28	492.8	243.7	500.6	238.7	509	232	456.3	177.7	429	141	75.5	121.2

Figure 19(a). Output data of the test results for the curve B with $\varepsilon = 0{\cdot}1$.

Biarc		Start point			End point			Centre			Radius
		x	y	z	x	y	z	x	y	z	r
biarc 1	arc 1	0	0	100	1.2	0	98.5	4.5	0	102.5	5.2
	arc 2	1.2	0	98.5	2.3	0	95.8	6.4	0	98.1	4.6
biarc 2	arc 1	2.3	0	95.8	4.4	0	93.1	14.5	0	102.8	14
	arc 2	4.4	0	93.1	7	0.1	88	14.8	0	92.8	9.1
biarc 3	arc 1	7	0.1	88	8.7	0.1	85.3	24.1	−0.1	98.5	20.1
	arc 2	8.7	0.1	85.3	11.4	0.2	81	24	−0.1	89.1	15
biarc 4	arc 1	11.4	0.2	81	13.1	0.2	78.4	32.2	−0.2	94.5	24.8
	arc 2	13.1	0.2	78.4	15.8	0.3	74.5	32.7	−0.3	86.2	20.6
biarc 5	arc 1	15.8	0.3	74.5	20.7	0.5	67.7	165.4	−5.3	178.3	182.2
	arc 2	20.7	0.5	67.7	30.6	0.8	52.7	55.3	−0.9	94.1	48.2
biarc 6	arc 1	30.6	0.8	52.7	36.1	−0.4	65.4	55.6	−14.7	94.5	51
	arc 2	36.1	−0.4	65.4	49.3	2.2	37.2	165	−54.3	175	188.5
biarc 7	arc 1	49.3	2.2	37.2	53.5	2.4	34.1	82.8	−14.2	77.2	54.6
	arc 2	53.5	2.4	34.1	54.9	2.6	32.5	56.8	0.5	39.1	7.2
biarc 8	arc 1	54.9	2.6	32.5	59.2	2.1	36.5	57.5	−2	4.18	10.8
	arc 2	59.2	2.1	36.5	61.9	3	28.2	80.6	−13.3	56.6	37.7
	...	...	...	...	...	...	...	...	...	...	...

Figure 19(b). A portion of the output data of the test results for the 3D surface C with $\varepsilon = 1.0$.

Acknowledgement

This research is supported in part by the National Science Council of Taiwan, ROC, under research project No. NSC-87-2213-E-155-023.

References

AUSTIN, S. P., JERARD, R. B. and DRYSDALE, R. L., 1997, Comparison of discretization algorithms for NURBS surfaces with application to numerically controlled machining. *Computer-Aided Design,* **29**, 71–83.

CHOI, B. K. and JUN, C. S., 1989, Ball-end cutter interference avoidance in NC machining of sculptured surfaces. *Computer-Aided Design,* **21**, 371–378.

ELBER, G. and COHEN, E., 1994, Toolpath generation for freeform surface models. *Computer-Aided Design,* **26**, 490–496.

HUANG, Y. and OLIVER, J. H., 1994, Non-constant parameter NC tool path generation on sculptured surfaces. *International Journal of Advanced Manufacturing Technology,* **9**, 281–290.

KIM, K. I. and KIM, K., 1995, A new machine strategy for sculptured surface using offset surface. *International Journal of Production Research,* **33**, 1683–1697.

JENSEN, C. G. and ANDERSON, D. C., 1996, A review of numerically controlled methods for finish-sculpture-surface machining. *IIE Transactions,* **28**, 30–39.

LEE, K., KIM, T. J. and HONG, S. E., 1994, Generation of toolpath with selection of proper tools for rough cutting process. *Computer-Aided Design,* **26**, 823–831.

LONEY, G. C. and OZSOY, T. M., 1987, Machining of free form surfaces. *Computer-Aided Design,* **19**, 85–90.

MEEK, D. S. and WALTON, D. J., 1992, Approximation of discrete data by G^1 arc splines. *Computer-Aided Design,* **24**, 301–306.

MEEK, D. S. and WALTON, D. J., 1993, Approximating quadratic NURBS curves by arc splines. *Computer Aided Design,* **25**, 371–376.

MORETON, D. N., PARKINSON, D. B. and WU, W. K., 1991, The application of biarc technique in CNC machining. *Computer Aided Engineering Journal,* **8**, 54–60.

ONG, C. J., WONG, Y. S., LOH, H. T. and HONG, X. G., 1996, An optimization approach for biarc curve-fitting of B-spline curves. *Computer-Aided Design,* **28**, 951–959.

PARKINSON, D. B. and MORETON, D. N., 1991, Optimal biarc-curve fitting. *Computer Aided Design,* **23**, 411–419.

SCHONHERR, J., 1993, Smooth biarc curves. *Computer-Aided Design,* **25**, 365–370.

TANG, K., CHEN, C. C. and DAYAN, Y., 1995, Offsetting surface boundaries and 3-axis gouge-free surface machining. *Computer-Aided Design,* **27**, 915–926.

TSENG, Y.-J. and SUE, Y.-R., 1999, Machining of free-form solids using an octree volume decomposition approach. *International Journal of Production Research,* **37**, 49–72.

YEUNG, M. K. and WALTON, D. J., 1994, Curve fitting with arc splines for NC toolpath generation. *Computer-aided Design,* **26**, 845–849.

YOU, C.-F. and CHU, C.-H., 1995, An automatic path generation method of NC rough cut machining from solid models. *Computers in Industry,* **26**, 161–173.